A crusher for single particle testing

A crusher for single particle testing

M. A. Verspui, G. de With, and E. C. A. Dekkers
Eindhoven University of Technology, P.O. Box 513, 5600 MB, Eindhoven, The Netherlands

(Received 13 June 1996; accepted for publication 11 November 1996)

For the investigation of particle failure in abrasive processes a single particle crusher has been developed. Basically the apparatus consists of two approaching diamond anvils between which a particle is positioned. Both the force and displacement can be either measured or controlled during an experiment. The force is determined by the current through the voice coil with a resolution of 0.5 mN. The vertical displacement of the lower anvil is measured by three inductive displacement transducers, each with a resolution of 0.1 μm. Single abrasive particles in the size range 10–500 μm can be used. The crushing process can be monitored through the upper anvil by a long distance microscope and recorded video. Preliminary experiments show that three different failure mechanisms can be distinguished: chipping, breaking, and fragmentation. By far the most dominant failure mechanism is chipping. The data of the crushing experiments are represented in a Weibull plot. The generally low value for the Weibull modulus indicates a large variability in strengths of the abrasive particles. [S0034-6748(97)00503-0]

I. INTRODUCTION

The elucidation on abrasive processes like two body abrasion, three-body abrasion, and erosion is rather complex since many parameters play a role. Removal rates depend on substrate properties (e.g., hardness, Young's modulus, fracture toughness), process parameters (e.g., relative speed, mode of operation) and powder properties (e.g., size, hardness, shape). Investigation on the influence of particle size and shape showed that during abrasion both the size and shape significantly change due to failure of the particles.[1] These changes in particle size and shape will on their turn influence the removal rate and resulting roughness. For a better understanding of the interaction between workpiece and abrasive particle a detailed study on particle strength and particle failure mechanisms is needed. For this purpose an apparatus for crushing experiments has been developed.

From the literature several methods are available for strength characterization of particles, powders, or granules.[2–12] In mill tests the grains are milled under specific conditions in a ball mill. The number of rotations is measured at which a certain amount of the grains has or has not failed.[2] In roll-crushers[3,4] particles are dropped one by one in a gap between two rolls. One cylinder is driven through a flexible coupling, the other is free to run. The grains are pulled between the rolls by friction and then crushed. The forces required to break the grains are measured with strain gauges. From the force readings different types of grain failure could be observed.[4]

For particle strength tests often compression tests are used.[5–10] In such a crushing apparatus a particle is placed between two parallel platens of a hard material. The particle will be loaded until failure and the force at failure will be determined. For slow compression tests on sand-cement and glass spheres Arbiter *et al.*[5] used a conventional hydraulic testing machine. Feng and Field[6] used an Instron 1122 machine with tungsten anvils for static strength tests on diamond grits. The loading rate was 0.05 mm/min. Yoshikawa and Sata[7] used parallel plates of sintered tungsten carbide and observed the process of fracturing with a microscope aligned perpendicular to the loading direction, using a loading rate of 71 g/s. Sikong *et al.*[8] used a modified dynamic ultramicro hardness tester (Shimadzu, DUH-50) with a maximum load of 0.98 N for their compression tests on some minerals and coals. The anvils were made of diamond. The compression load was controlled with an accuracy of 1%. The displacement of the specimen in the loading direction was measured by a differential transformer with a sensitivity of 0.01 μm. For strength tests on abrasive grains Takazawa[9] used a simple apparatus with sintered carbide lower anvils and a diamond with a flat side as upper anvil. The abrasive grain ground flat at the bottom was placed on the lower anvil. The fracture load and compressive displacement were measured and recorded by pen-writing. All crushers discussed above, except for the ultramicro hardness tester of Sikong *et al.*[8] (1–800 μm) were used for relatively large powders (0.5–25 mm).

Schönert and Rumpf[10] gave a very detailed description of two particle crushers they used for the investigation on the behavior of small particles (10–1000 μm) under compression. One crusher had a maximum load of 2 kg and the other one of 100 kg. The crushers were based on an electromagnetic system. The anvils were made of sapphire. The upper anvil was attached to a stronger glass plate. Through this glass plate and the upper anvil the particle could be observed during compression. For the collection of the debris, they performed the test in a drop of water. From the tests the compression strength and the energy required for crushing was calculated. Also the particle size distribution and the surface of the debris were examined.

Compression tests have also been done on granules as used in powder processing. Coupelle *et al.*[11] described an apparatus based on a stepping motor which displaces the lower anvil. The displacement of the lower anvil is measured by an inductive transducer and the force by a strain gauge. Van der Zwan[12] reported also on the strength of granules using a simple device constructed on an electronic balance.

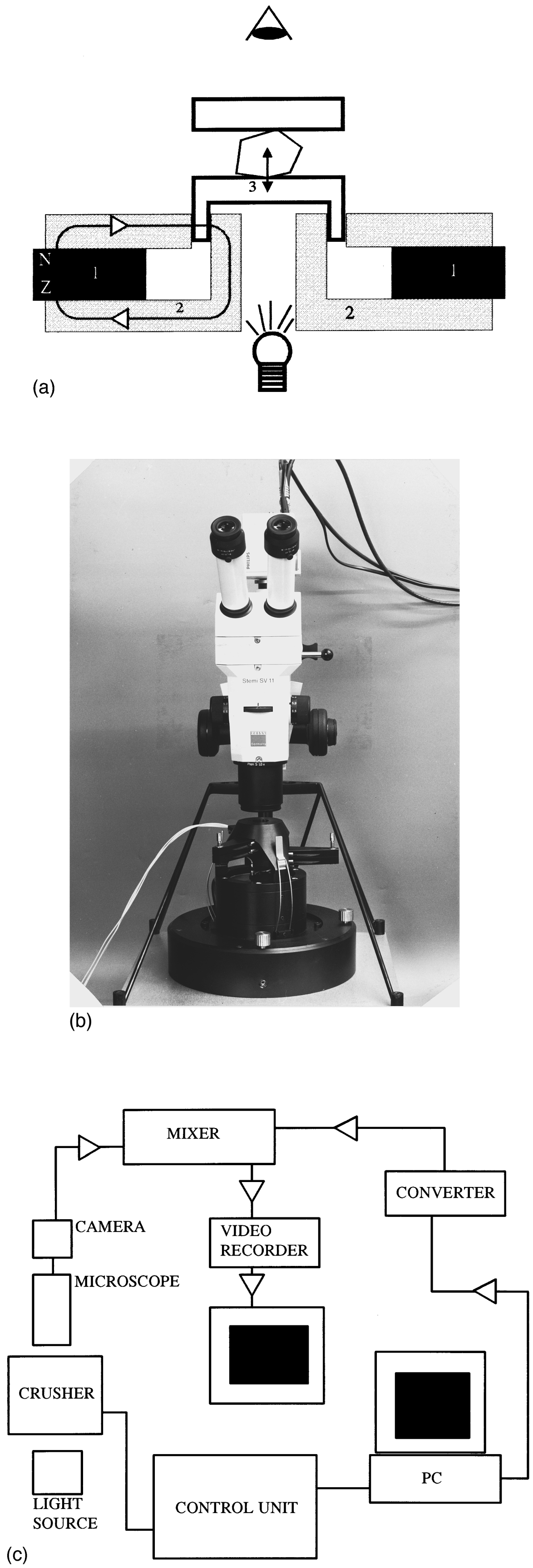

FIG. 1. (a) Schematic representation of the part of the crusher with the ring magnet and the voice coil: (1) ring magnet, (2) ferrous core, (3) voice coil/anvil, and (4) gap. (b) Photo of the single particle crusher. (c) Simplified scheme of the equipment.

TABLE I. Advantages and disadvantages of the design.

Advantages	Disadvantage
Force is directly proportional with current	efficiency low at low velocities
Current can be used as force signal	
Fast movements because of low mass	
Large bandwidth	
Large force at relatively low current	
No friction	

Both papers show a clear influence of process variables on the strength of granules.

II. THE SINGLE PARTICLE CRUSHER

The single particle crusher we developed for the investigation of single abrasive particles in the size range of 10–500 μm resembles the crusher described by Schönert and Rumpf.[10] For the small translations required, use was made of a voice coil, schematically shown in Fig. 1(a). The voice coil consists of a permanent ring magnet with ferrous core and upper plate. The field lines have the direction as shown in Fig. 1(a). The voice coil is positioned in the gap. When a current flows through the coil, a Lorenz force, proportional with the current, acts on the coil in an axial direction.[13] The advantages and disadvantages of the design are given in Table I. Figure 1(a) shows schematically the part of the crusher with the ring magnet and the voice coil.

The lower diamond anvil is positioned on the voice coil and will displace upwards when a current runs through the coil. The force on the coil (and on the anvils) is given by:

$$F_c = B_g I_c l_w$$

with $I_c =$ current through the coil $[A]$, $l_w =$ length of wire in the field $[m]$ and $B_g =$ magnetic flux in the gap $[T]$. The exact relative displacement between the lower and upper anvil is determined independently from the force with three inductive high speed displacement transducers. A photograph of the single particle crusher is given in Fig. 1(b). Easy to recognize is the ring magnet on the bottom of the picture. The anvils, two transparent parallel diamond cylinders, are positioned in the center of the crusher. The stereomicroscope placed on top of the crusher enables one to make observations during the crushing experiment. The force signal is superposed on the microscope image by a digital signal mixer. The resulting image is recorded on a video tape. This makes it possible to classify the mechanisms of failure at each peak load in the force signal. A simplified scheme of the equipment is given in Fig. 1(c). In Table II the specifications of the single particle crusher are summarized.

TABLE II. The specifications of the crusher.

Specifications	Range	Accuracy
Particle size	10–500 μm	⋯
Displacement	0–500 μm	0.1 μm
Force	0–50 N	0.5 mN
Velocity	0.1–1000 μm/s	⋯

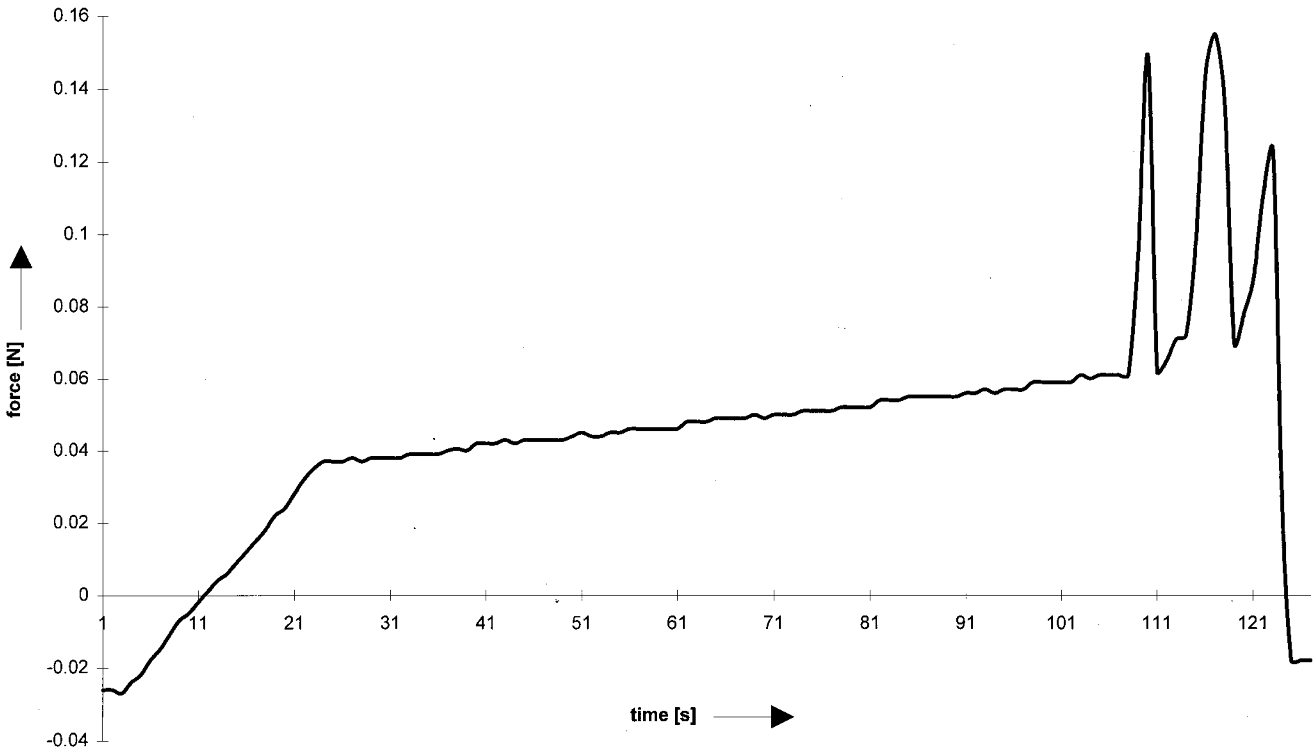

FIG. 2. Example of a force signal. Due to the elasticity of the activator (membrane) the force will slowly increase during the crushing tests, as is illustrated by the line with the flat slope before the particle is crushed.

A single particle is placed on the lower anvil and then crushed. The strength test can be executed in air, in water, or on a thin and soft foil. It is also possible to collect the debris after crushing. An example of a force signal of a particle crushed in air is given in Fig. 2. When a piece detaches from the particle the force will reduce to zero. As a result of the released elastic energy build up in the apparatus, the anvils tend to accelerate, risking a collision of the anvils. To avoid a collision the stiffness of the drive system has been maximized. The stiffness of the system is determined by the motion feedback control and restricted by the displacement measurement. The direct measurement of the displacement between the two anvils with contactless sensors makes sure that the displacement measurements are force independent.

Since the force is determined by the current through the coil, the slide guidance of the voice coil with the lower anvil has to be completely friction free. For the relatively small displacements demanded this has been realized by five elastically deforming rods positioned tangentially around the coil. Every rod controls one degree of freedom in its axial direction, resulting in five fixed degrees of freedom. The axial degree of freedom of the voice coil has not been fixed, providing a hysteresis free slide guidance for small displacements. The slide guidance provides perfect reproducibility and thermal stability because of the statically determined design.

TABLE III. Mean force, stress, and Weibull moduli for Al_2O_3 F240; $s(\overline{F})$ is the sample standard deviation, $s(F_0)$ and $s(m)$ are the standard deviations of the characteristic force and the Weibull modulus, respectively.

	Mean $\overline{F}$ [a]	$s(\overline{F})$	F_0 [a]	$s(F_0)$	$m[-]$	$s(m)$	Number of particles
Force [N]	0.36	0.41	0.348	0.036	1.05	0.11	84
Stress [MPa]	338.64	435.69	291.84	38.49	0.80	0.08	84

[a]The characteristic force F_0 is the force at a failure probability of 63%. The mean $\overline{F}$ is related to F_0 by $\overline{F}=(1/m)!F_0$.

III. PRELIMINARY EXPERIMENTS

With the single particle crusher some preliminary tests have been performed on Al_2O_3 particles with a mass modal diameter of 44.2 μm. Figure 2 represents an example of a force signal. For each particle the first peak in the force signal has been determined. In Fig. 3(a) all the fracture forces are plotted in a Weibull plot, where the failure probability P_f is given by the empirical relation:

$$\ln \ln \left(\frac{1}{1-P_f}\right)=m \ln \left(\frac{F}{F_0}\right)+ \ln R,$$

with $F=$ force at failure, F_0 is the characteristic force, indicating a failure probability of 63%, and $m=$ the Weibull modulus. The variability in strength increases with a decreasing value for m. For a data set which can reasonably be described with Weibull statistics, a plot of $\ln \ln (1/1-P_f)$ vs $\ln F$ results in a straight line with slope m and intercept $\ln R$. The low value for m in Fig. 3(a) indicates a high variability in fracture force of the particles. Reasons for this high variability may be the size variation in the particles, the variability in particle shape, and particle orientation on the lower

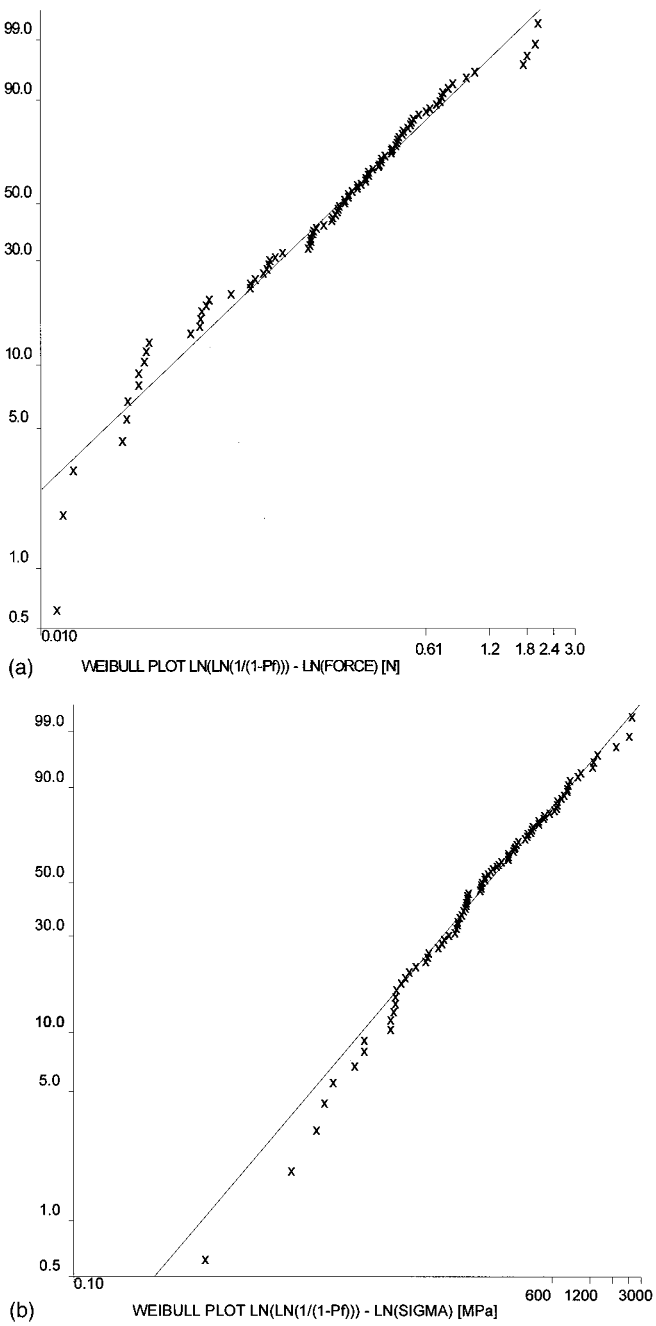

FIG. 3. (a) Weibull plot of the fracture forces of Al_2O_3 F240. (b) Weibull plot of the fracture stresses of Al_2O_3 F240.

anvil. Furthermore, the crystallographic orientation and the alignment of different crystal planes with respect to the anvils may influence the variability in fracture force. The influence of the distributed sizes can be partially obviated by plotting the fractures stresses instead of the fracture forces. One way to convert fracture loads to fracture stress is given by Hiramatsu and Oka.[14] They proposed:

$$\sigma_f = \frac{2.8F}{\pi d_f^2},$$

where $\sigma_f =$ fracture stress, $F =$ load at fracture, and $d_f =$distance between anvils at the moment of fracture. Other possibilities use information of the projected particle image. The vices and virtues of these methods will be discussed elsewhere.[15]

The stresses for the Al_2O_3 particles, calculated from the equation of Hiramatsu and Oka are also represented in a Weibull plot, as shown in Fig. 3(b). The mean force $\overline{F}$ and stress $\overline{\sigma_0}$ and the Weibull moduli of the plots in Fig. 3 are given in Table III. The low value of the Weibull moduli for the force remain after conversion to stress and indicates a large intrinsic variability in strengths.

Analysis of the video images, obtained during the preliminary experiments show that three different types of failure can be identified:

(i) chipping: small pieces detach from the particle;
(ii) breaking: a particle breaks in a few large pieces;
(iii) fragmentation: a particle breaks in many small pieces.

Far the most dominant mechanism of failure was chipping (72%). Less particles (27%) broke in two or three large pieces. Exceptionally (1%) fragmentation occurred.

IV. FINAL REMARKS

Future experiments will include crushing experiments using various types of powders with varying sizes and an analysis of their strength and failure mechanisms. Hopefully, these data, accompanied by some fractography studies, will gives us more insight into the failure mechanisms of particles in abrasive processes. However, it is also possible to test other particulate materials, e.g., granulates.

ACKNOWLEDGMENTS

The authors thank M. H. C. Janssen for tuning up the control unit. They also thank E. van Gessel, who performed most of the experiments.

[1] M. A. Verspui, G. de With, P. G. Th van der Varst, and M. Buijs, Wear **188**, 102 (1995).
[2] L. Höhne, C. Ullner, and G. Kley, Wear **151**, 195 (1991).
[3] J. Larsen-Basse, Wear **166**, 93 (1993).
[4] J. N. Brecker, J. Eng. Ind. **96**, 1253 (1974).
[5] N. Arbiter, C. C. Harris, and G. A. Stamboltzis, Soc. Min. Eng., Trans. A. I. M. E. **244**, 118 (1969).
[6] Z. Feng and J. E. Field, Ind. Diamond Rev. p. 104 (1989).
[7] H. Yoshikawa and T. Sata, Sci. Papers I. P. C. R. **54**, 389 (1960).
[8] L. Sikong, H. Hashimoto, and S. Yashima, Powder Tech. **61**, 51 (1990).
[9] K. Takazawa, Proceedings of the International Grinding Conference, Pittsburgh, 1972, pp. 75–90.
[10] K. Schönert and H. Rumpf, Symposium Zerkleinern, Frankfurt am Main, 1962, pp. 108–127.
[11] P. Coupelle, J. Destermes, F. Miglioretti, and J. F. Baumard, *Deformation Des Granules d'Atomisation Sous Compression Uniaxiale* (L'Industrie Céramique, 1991), Vol. 861, pp. 408–412.
[12] J. van der Zwan, *Granule Strength and Compaction Behaviour of Agglomerated Materials*, *Euroceramics 1*, edited by G. de With, R. A. Terpstra, and R. Metselaar (Elsevier, London, 1989), pp. 238–242.
[13] E. C. A. Dekkers, Mikroniek **35**, 129 (1995) (in Dutch).
[14] Y. Hiramatsu and Y. Oka, Int. J. Rock Mech. Min. Sci. **3**, 89 (1966).
[15] M. A. Verspui and G. de With (in preparation).